

Structural responses of a fluid-loaded cylinder/plate structure using deterministic and statistical approaches

Hongjian Wu (1), Nicole Kessissoglou (1), Brian Mace (2)

(1) School of Mechanical and Manufacturing, University of New South Wales, Sydney, Australia

(2) Department of Mechanical Engineering, University of Auckland, Auckland, New Zealand

ABSTRACT

This work studies the dynamic responses of a coupled fluid-loaded cylinder/plate structure. The cylindrical shell closed at each end by circular plates is driven by an axial force applied centrally to one end plate, resulting in an axisymmetric case. Analytical expressions for the axial and radial displacements of the cylindrical shell are derived. The spatially and frequency averaged energy due to radial motion of the cylindrical shell is compared with results obtained from a Statistical Energy Analysis (SEA) model. Results from a fully coupled finite element /boundary element (FE/BE) model are also presented. The dynamic responses estimated by the deterministic and stochastic approaches are discussed.

INTRODUCTION

Vibration characteristics of cylindrical shells in the low frequency range have been investigated by many researchers. Most of the thin shell theories and fundamental partial differential equations for thin cylindrical shells have been summarized by Leissa (1993). The dynamic characteristics of coupled cylinder/plate structures have been investigated by several authors (Irie et al. 1984, Huang and Soedel 1993, Tso and Hansen 1995). The presence of a dense fluid medium results in strong fluid-structure interaction. Cylindrical shells with internal or external fluid loading have been examined by Fuller and Fahy (1982) and Scott (1988). A general technique combining a classic in vacuo eigenfunction expression with Green's function method accounting for fluid loading was used to obtain the vibratory response of a finite fluid-loaded cylindrical shell under harmonic excitation (Stepanishen 1982). The approximate analytical expressions for velocity responses induced by axisymmetric wave propagating along the fluid-loaded cylindrical shell were compared with numerical results below the ring frequency (Photiadis 1990). A Fourier integral transform method was implemented to generalise the surface velocity distribution on a fluid-loaded cylindrical shell closed with rigid end closures (Sandman 1976). A wave propagation approach was used to conduct the frequency analysis of submerged finite cylindrical shells enclosed with plate end-caps in comparison with FEM/BEM method (Zhang 2002). The first eight coupled natural frequencies were obtained with good agreement between the wave propagation and the numerical methods.

Statistical Energy Analysis (SEA) is an energy based technique to predict the average noise and vibration levels of complex structures at high frequencies (Fahy 1994, Lyon 1995). Tso and Hansen (1997) used SEA to predict structure-borne noise transmission in naval ship structures. External fluid load can be modelled as an additional subsystem in SEA in order to consider fluid-structure interaction. Liu and Keane (2000) studied the vibrations of a coupled fluid-structural pipework system utilising SEA method. Manning (2002)

implemented SEA method to predict the vibrational energy transmission from fluid-filled piping systems. Three modifications were made to initial SEA models: introducing the frequency-dependent damping loss factors, reducing the coupling between pipe bending and inplane modes, and adding the coupling between the pipe and the support structure. The comparison between refined SEA model and test data provided better accuracy of the SEA predictions.

Cylindrical shells used in engineering applications such as pressure vessels, autonomous underwater vehicles and submarine hulls are generally subjected to loads. For example, a submarine hull is excited by the propulsion system and on-board machinery. Fluctuating forces arise from the rotation of the propeller in a non-uniform wake field. Harmonic forces also arise from the motion of rotary parts in the diesel engines, generators and auxiliary equipment. All these loads generate vibration in the mid frequency range where neither deterministic nor statistical approaches alone are suitable. To address this shortcoming in mid frequency predictive techniques, hybrid deterministic-statistical methods for vibration analyses of structures have been developed (Cotoni et al. 2007, Langley and Bremner 1999, Langley and Cordioli 2009). Using the hybrid FE-SEA technique, rigid body components are modelled using finite elements while the flexible components are modelled using SEA.

In this paper, analytical and numerical models are developed for a coupled fluid-loaded cylinder/plate structure, corresponding to a cylindrical shell closed by either rigid or flexible circular plates at each end. The system is driven by an external axial force at one end plate, resulting in only axisymmetric motion of cylindrical shell. The frequency responses and vibrational energy levels of the cylinder/plate structure are presented for both the in-vacuo and fluid-loaded cases. The dynamic responses obtained from the analytical model are validated with results from a fully coupled FE/BE model. The geometry of the structure in the finite element model was then imported into an SEA software package as the structural subsystem. The spatially and frequency aver-

aged energy levels of the cylinder obtained analytically are compared to results obtained from the SEA model. The dynamic responses from the deterministic and statistical approaches are discussed.

ANALYTICAL MODEL

Dynamic response of a fluid-loaded cylindrical shell

In this work, a fluid-loaded cylindrical shell closed with circular end plates is modelled. Both flexible and rigid end plates are considered. An axial force is applied at the centre of one end plate, as shown in Fig. 1. The cylindrical shell has length L and is assumed to be thin-walled, that is, the shell thickness h is much smaller than the mean shell radius a . The material parameters for the cylindrical shell are denoted by Young's modulus E , Poisson's ratio μ , and mass density ρ . In Fig. 2, the shell motions are represented by u_c , v_c and w_c which are, respectively, the displacements in the longitudinal x , tangential θ and radial z directions.

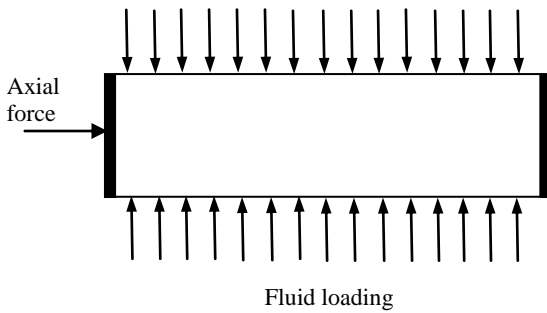


Figure 1. Schematic diagram of the fluid loaded cylinder with rigid end plates and under axial excitation

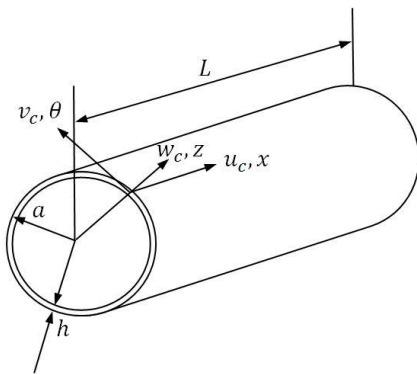


Figure 2. Displacements and co-ordinate system of a cylindrical shell

The axial force applied at the centre of one end gives rise to an axisymmetric case corresponding to excitation of the zeroth circumferential modes ($n=0$) of the shell. For the $n=0$ circumferential modes, the equations of motion for the axial and radial shell displacements become uncoupled from the equation of motion for circumferential motion. Using Flügge's theory, the equations of motion for the axial and radial displacements of the fluid-loaded cylindrical shell are given by (Flügge 1973, Leissa 1993)

$$\frac{\partial^2 u_c}{\partial x^2} + \frac{\mu}{a} \frac{\partial w_c}{\partial x} - \beta^2 a \frac{\partial^3 w_c}{\partial x^3} - \frac{1}{c_L^2} \frac{\partial^2 u_c}{\partial t^2} = 0 \tag{1}$$

$$\beta^2 \left(a^2 \frac{\partial^4 w_c}{\partial x^4} - a \frac{\partial^3 u_c}{\partial x^3} \right) + \frac{\mu}{a} \frac{\partial u_c}{\partial x} + \frac{(1+\beta^2)}{a^2} w_c + \frac{1}{c_L^2} \frac{\partial^2 w_c}{\partial t^2} - \frac{1}{c_L^2} \frac{p_a}{\rho h} = 0 \tag{2}$$

where $c_L = \sqrt{E / \rho(1-\mu^2)}$ is the longitudinal wavespeed. $\beta = h / \sqrt{12} a$ is a non-dimensional thickness parameter. Equation (2) includes the fluid-loading term $-p_a / \rho h c_L^2$ due to the acoustic pressure p_a . The acoustic pressure due to the fluid loading acting normally to the surface of the shell is approximated using an infinite model and is expressed by (Junger and Feit 1986)

$$p_a = -(r_f - j\omega m_f) \frac{\partial w_c}{\partial t} \tag{3}$$

where ω is the radian frequency. The fluid reactance m_f and fluid resistance r_f per unit area are given by (Junger and Feit 1986)

$$\left. \begin{aligned} m_f &= \rho_f a \frac{K_0(\beta_s)}{\beta_s K_1(\beta_s)} \\ r_f &= 0 \end{aligned} \right\}, \quad k_s > k_f \tag{4}$$

$$\left. \begin{aligned} m_f &= \rho_f a \frac{J_0(\beta_f)J_1(\beta_f) + Y_0(\beta_f)Y_1(\beta_f)}{\beta_f |H_1(\beta_f)|^2} \\ r_f &= \frac{2\rho_f c_f k_f a}{\pi \beta_f^2 |H_1(\beta_f)|^2} \end{aligned} \right\}, \quad k_s < k_f \tag{5}$$

where $\beta_s = a\sqrt{k_s^2 - k_f^2}$ and $\beta_f = a\sqrt{k_f^2 - k_s^2}$. ρ_f is the density of the fluid and c_f is the speed of sound in the fluid. k_s is the axial wavenumber of the structure and k_f is the wavenumber of the fluid. J_n and Y_n are respectively the Bessel functions of the first and second kind, of order n . K_0 and K_1 are respectively the modified Bessel function of the second kind of order zero and order one. H_1 is the Hankel function of the order one. General solutions to the cylindrical shell displacements are of the form

$$u_c(x,t) = U_c e^{jk_s x} e^{-j\omega t} \tag{6}$$

$$w_c(x,t) = W_c e^{jk_s x} e^{-j\omega t} \tag{7}$$

U_c and W_c are respectively the wave amplitudes in the axial and radial directions. Substituting these general solutions into the equations of motion gives rise to the following matrix expression

$$\begin{bmatrix} \Omega^2 - a^2 k_s^2 & -j(\beta^2 a^3 k_s^3 + \mu a k_s) \\ j(\beta^2 a^3 k_s^3 + \mu a k_s) & \beta^2 a^4 k_s^4 + 1 + \beta^2 - \tau \Omega^2 \end{bmatrix} \begin{bmatrix} U_c \\ W_c \end{bmatrix} = \begin{bmatrix} 0 \\ 0 \end{bmatrix} \quad (8)$$

where

$$\tau = 1 + \frac{m_f}{\rho h} + \frac{j r_f}{\omega \rho h} \quad (9)$$

$\Omega = \omega a / c_L$ is the non-dimensional ring frequency, where the ring frequency ($\omega_r = c_L / a$) is the frequency at which the wavelength of extensional waves in the shell is equal to the shell circumference. Putting the determinant of the matrix in equation (8) to zero yields the following characteristic equation of the system

$$-\beta^2 a^6 k_s^6 + (\beta^2 a^4 \Omega^2 - \beta^4 a^6 - \mu \beta^2 a^4) k_s^4 - (1 + \beta^2 - \tau \Omega^2 + \mu \beta^2 a^2 + \mu^2) a^2 k_s^2 + (1 + \beta^2 - \tau \Omega^2) \Omega^2 = 0 \quad (10)$$

which is a third order dispersion equation in terms of k_s^2 . Due to the Hankel and Bessel functions, the characteristic equation given by equation (10) is non-linear and the complex axial wavenumbers can only be determined using a numerical method (Scott 1988). For the in vacuo case, the characteristic equation is a polynomial of sixth order in terms of k_s . Three couples of complex conjugated solutions are determined as complex axial wavenumbers. The complex wavenumber can be written as $k_s = k_{real} + j k_{imag}$. Similarly, the characteristic equation can be written as $C = C_{real} + j C_{imag}$. The complex solutions of the characteristic equation can then be found by solving $\{C_{real}(k_{real}, k_{imag}) = 0; C_{imag}(k_{real}, k_{imag}) = 0\}$. The axial wavenumbers are determined for any value of real frequency ω as described by Scott (1988).

Omitting the time dependent term $e^{-j\omega t}$ for harmonic motion, the complete solutions can be written as:

$$u_c(x) = \sum_{i=1}^6 U_{c,i} e^{j k_{s,i} x} \quad (11)$$

$$w_c(x) = \sum_{i=1}^6 W_{c,i} e^{j k_{s,i} x} \quad (12)$$

$U_{c,i}$ and $W_{c,i}$ are determined from the boundary conditions. In the presence of a heavy fluid medium, the solutions for the cylindrical shell displacements are more accurate in the low frequency range where the fluid wavenumber k_f is higher than the structural wavenumber k_s .

Dynamic response of a circular plate

The equations of motion for the bending (out-of-plane) w_p and in-plane u_p displacements of a circular plate in axisymmetric motion are given by (Tso and Hansen 1995)

$$\nabla^4 w_p - \left(\frac{\rho_p \omega^2 h_p}{D_p} \right) w_p = 0 \quad (13)$$

$$\frac{\partial^2 u_p}{\partial r^2} + \frac{1}{r} \frac{\partial u_p}{\partial r} - \frac{\rho_p (1 - \mu_p)}{E_p} \frac{\partial^2 u_p}{\partial t^2} = 0 \quad (14)$$

$\nabla^4 = \nabla^2 \nabla^2$ where ∇^2 is the Laplacian operator for axisymmetric motion, $D_p = E_p h_p^3 / 12(1 - \mu_p^2)$ is the plate flexural rigidity, and ρ_p , h_p , E_p , μ_p are the plate density, thickness, Young's modulus and Poisson's ratio, respectively. r is the radial coordinate from the plate centre. Fluid loading on the end plates has been neglected. General solutions for the bending and in-plane displacements in harmonic motion are given by (Tso and Hansen 1995)

$$w_p = A_1 J_0(k_{pB} r) + A_2 I_0(k_{pB} r) \quad (15)$$

$$u_p = B_1 \frac{\partial J_0(k_{pL} r)}{\partial r} \quad (16)$$

where J_0 is the Bessel function of the first kind of order zero and I_0 is the modified Bessel function of the first kind of order zero. k_{pB} and k_{pL} are respectively the bending and in-plane structural wavenumbers. For an annular plate in axisymmetric motion, the general solutions for bending and in-plane motion are given by (Tso and Hansen 1995)

$$w_a = A_1 J_0(k_{pB} r) + A_2 I_0(k_{pB} r) + A_3 Y_0(k_{pB} r) + A_4 K_0(k_{pB} r) \quad (17)$$

$$u_a = B_1 \frac{\partial J_0(k_{pL} r)}{\partial r} + B_2 \frac{\partial Y_0(k_{pL} r)}{\partial r} \quad (18)$$

where Y_0 is the Bessel function of the second kind of order zero and K_0 is the modified Bessel function of the second kind of order zero. Putting the coefficients A_3 , A_4 and B_2 in equations (17) and (18) to zero reduces the general solutions to those of a circular plate given by equations (15) and (16).

Cylindrical shell closed by rigid end plates

Using rigid end plates, the boundary conditions at each end of the cylinder corresponding to $x=0$ and $x=L$ result in the radial displacement and slope of zero (Leissa 1993)

$$w_c = 0, \quad \frac{\partial w_c}{\partial x} = 0 \quad (19,20)$$

The external excitation was modelled as an axial force of amplitude F_{ext} at one end of the cylinder corresponding to $x=0$. The force equations at $x=0$ and $x=L$ are given by

$$F_{ext} + 2\pi a F_{x,c} = m \frac{\partial^2 u_c}{\partial t^2}; \quad x=0 \quad (21)$$

$$-2\pi a F_{x,c} = m \frac{\partial^2 u_c}{\partial t^2}; \quad x=L \quad (22)$$

where m is the mass of each rigid end plate. $F_{x,c}$ is the internal axial force of the cylinder per unit length of circumference and is given by (Leissa, 1993)

$$F_{x,c} = -\frac{Eh}{1 - \mu^2} \left(\frac{\partial u_c}{\partial x} + \frac{\mu}{a} w_c - \beta^2 \frac{\partial^2 w_c}{\partial x^2} \right) \quad (23)$$

Cylindrical shell closed by flexible end plates

In the case of flexible end plates, the point force is applied axially at the centre of the end plate located at $x=0$. This was analytically modelled by separating the circular plate at $x=0$ into an inner circular plate of radius a_1 and an outer annular plate of radius a_2 (Caresta and Kessissoglou 2011). The point force at the centre of the end plate was then approximated by a distributed force applied axially to the circumference of the inner circular plate, that is, at the junction of the annular and circular plates. Using a very small value for a_1 , the distributed force converges to a point force. The continuity equations between the circular and annular plates at $r = a_1$ are given by:

$$w_p = w_a, \quad u_p = u_a, \quad \frac{\partial w_p}{\partial r} = \frac{\partial w_a}{\partial r} \quad (24-26)$$

$$F_{x,p} + F_{x,a} = \frac{F_{ext}}{2\pi a_1} \quad (27)$$

$$F_{r,p} + F_{r,a} = 0 \quad (28)$$

$$M_p - M_a = 0 \quad (29)$$

The subscript ‘p’ denotes circular plate and the subscript ‘a’ denotes the annular plate. The positive directions of the forces, moments, displacements and slopes for the cylindrical shell and circular plates located at $x=0$ is shown in Fig. 3.

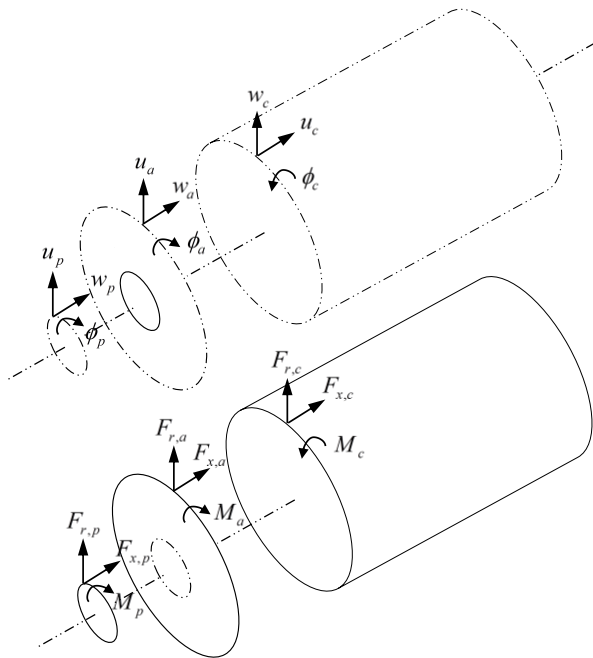


Figure 3. Displacements, slopes, forces and moments of the cylindrical shell and circular/annular plates

The corresponding expressions for the internal forces and moments of the cylindrical shell and plates are given in the Appendix. The continuity expressions between the annular plate and cylindrical shell at $x=0$ and $r = a_2$ (and noting

that a_2 is the same as the radius of the cylindrical shell, that is, $a_2 = a$) are given by:

$$u_c = w_a, \quad w_c = u_a, \quad \frac{dw_c}{dx} = -\frac{\partial w_a}{\partial r} \quad (30-32)$$

$$F_{x,c} + F_{x,a} = 0, \quad F_{r,c} + F_{r,a} = 0, \quad M_c - M_a = 0 \quad (33-35)$$

Similar equations to those given by equations (30) to (35) are used at the junction between the cylindrical shell and circular plate at $x=L$. The displacements, slope, forces and moment terms associated with the annular plate are replaced by those for a full circular plate.

For the structure consisting of a cylindrical shell closed with rigid end plates, there are a total of 6 unknown coefficients corresponding to the wave amplitudes of the cylinder displacements. For a cylindrical shell closed with flexible end plates, there are a total of 18 unknown coefficients for the cylinder and circular/annular plates. The various boundary and continuity equations at each end of the cylinder can be arranged in matrix form $\mathbf{B}\mathbf{X} = \mathbf{F}$, where \mathbf{X} is the vector of the unknown displacement coefficients and \mathbf{F} is the force vector containing only one non-zero term due to the external force. Solutions for the unknown coefficients of vector \mathbf{X} are determined by $\mathbf{X} = \mathbf{B}^{-1}\mathbf{F}$. The cylindrical shell axial and radial displacements are then obtained using equations (11) and (12) for the two cases using the rigid and flexible end plates.

FE/BE NUMERICAL MODEL

A finite element model of the coupled cylinder/plate structure was developed in MSC Patran/Nastran with a quadrilateral mesh using quad8 elements. The boundary conditions and external load were chosen to simulate those in the analytical model. The external fluid domain is modelled using the BEM module of the ESI Group VA-One 2010 software. A harmonic analysis was carried out and the frequency response results from the FE/BE model were validated against those obtained analytically.

STATISTICAL ENERGY ANALYSIS

Statistical Energy Analysis (SEA) is an energy based method in which a structure is decomposed into subsystems which contain a fairly uniform response in terms of their vibrational energy. Using SEA, a structure is modelled using only a few degrees of freedom, where each degree of freedom corresponds to a subsystem. The interaction between the SEA subsystems is based on the principle of conservation of the energy flow. In an SEA model, the power balance equations at each band-centre frequency over the frequency range of interest considers the power input to each subsystem due to external excitation, the power dissipated via damping in each subsystem, and the power transmitted between subsystems. The standard SEA equation which states the power balance for each subsystem in terms of the mean subsystem energies has the following well-known form (Fahy 1994, Lyon 1995)

$$P_{in,i} = \omega \eta_i E_i + \omega \sum_{j \neq i} \eta_{ij} n_i \left(\frac{E_i}{n_i} - \frac{E_j}{n_j} \right) \quad (36)$$

where $P_{m,i}$, E_i , n_i and η_i are respectively the input power, vibrational energy, modal density, and damping loss factor of subsystem i . η_{ij} is the coupling loss factor between subsystem i and subsystem j . Validity of the SEA equations is dependent, amongst other things, on there being weak coupling between the subsystems (Mace 1994).

The geometry of the coupled cylinder/plate structure developed in MSC Patran/Nastran was imported into the SEA module of the ESI Group VA-One 2010 software. The structure was decomposed into three structural subsystems corresponding to the cylindrical shell and two end plates. The fluid loading effect is simulated by connecting a semi-infinite-fluid (SIF) subsystem with the cylindrical shell subsystem in VA-One 2010 software. The power was injected into one end plate as shown in Fig. 4.

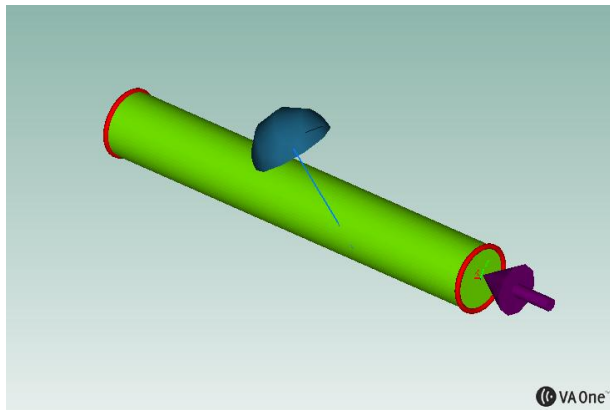


Figure 4. SEA model of the cylinder/plate structure showing input power at one end plate

RESULTS AND DISCUSSION

The cylinder of radius $a = 3.25\text{m}$, thickness $h = 0.04\text{m}$ and length $L = 45\text{m}$ is made of steel with Young's modulus $E = 2.1e11\text{N/m}^2$, Poisson's ratio $\mu = 0.3$ and density $\rho = 7800\text{kg/m}^3$. The structural damping loss factor was introduced analytically using a complex Young's modulus $E = E(1 - j\eta)$, where $\eta = 0.01$ is the structural loss factor. The mass of the cylinder is $M = 2.866e5\text{ kg}$. The additional mass of $m = 2e5\text{kg}$ for each rigid end plate was modelled using a very high Young's modulus of $E_p = 2.1e21\text{N/m}^2$ and mass density $\rho_p = 1.507e5\text{kg/m}^3$. The flexible end plates were modelled using the same Young's modulus and density as the cylindrical shell. The thickness and Poisson's ratio of the end plates were the same as for the cylindrical shell.

An axial force of 1N was applied to the centre of one end plate. Due to the excitation, only axisymmetric motion of the hull was considered in the analytical and computational models.

The analytical results were obtained using Matlab. The computational results were obtained using the FEM/BEM solver in the VA-One software. The SEA results were also obtained using the SEA solver in the VA-One software.

Frequency response

To validate the deterministic models, results for the frequency responses from the analytical and FE/BE methods are initially presented. The same dimensions and material properties of the cylindrical shell and end plates were used in both deterministic models. The frequency response function of the cylinder axial displacement is measured at the outer edge of the end plate at $x = 0$. Figures 5 and 6 present results for the cylinder closed by rigid end plates and flexible end plates, respectively. In both figures, results for both the in-vacuo case and with fluid-loading are given. Axial excitation at the centre of the end plate gives rise to an axisymmetric case in which only the zeroth circumferential shell modes ($n = 0$) are excited. The peaks in the frequency responses correspond to axial resonances at which the cylinder is in breathing motion. For this axisymmetric case, the effect of fluid loading reduces the peaks at the resonant frequencies, thus acting as a damping effect.

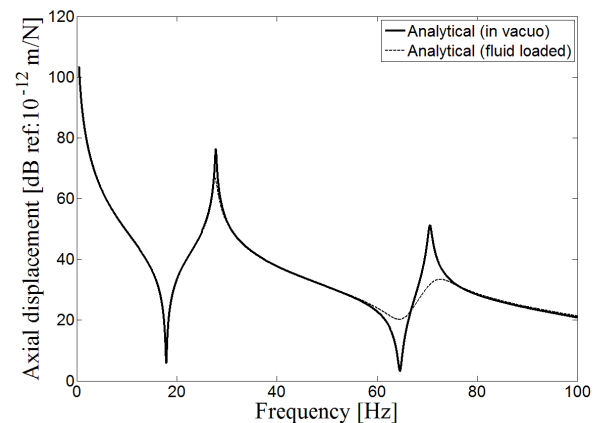


Figure 5. Axial displacement of the cylinder closed by rigid end plates, without and with fluid loading

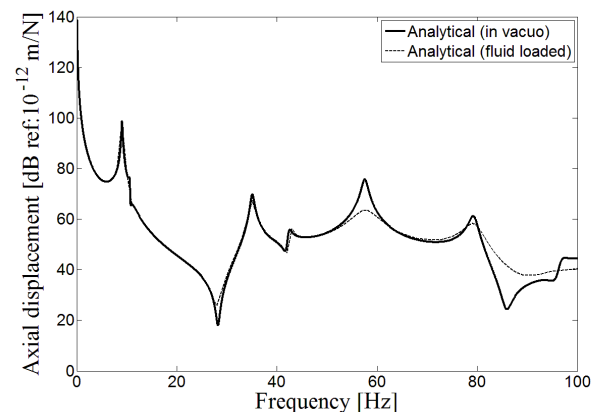


Figure 6. Axial displacement of the cylinder closed by flexible end plates, without and with fluid loading

Figures 7 and 8 compare results obtained analytically and from the FE/BE model, for the fluid-loaded cylinder with rigid and flexible end plates, respectively. Good agreement is observed at lower frequencies. The results start to deviate in amplitude at higher frequencies which is attributed to differing underlying assumptions associated with the fluid loading in the analytical and numerical models. In the analytical

model, fluid loading is only associated with travelling waves in the shell, whereas the FE/BE model considers fully coupled fluid-structure interaction.

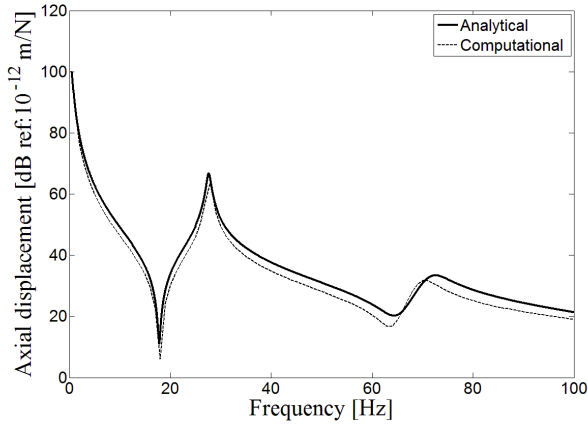


Figure 7. Axial displacement of the fluid-loaded cylinder closed by rigid end plates

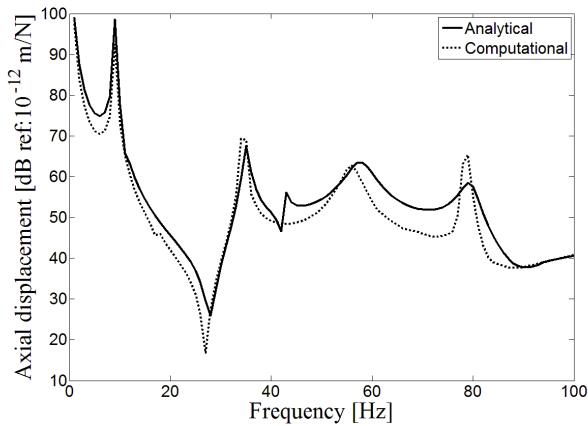


Figure 8. Axial displacement of the fluid-loaded cylinder closed by flexible end plates

Subsystem energy

A comparison between the analytical and SEA results was conducted by comparing the total energy levels of the cylinder. For the coupled cylinder/plate structure excited at one end, the transmission of vibrational energy is dominated by the radial (out-of-plane) motion (Tso and Hansen 1995). The spatially-averaged mean square radial velocity is obtained as

$$\langle \dot{w}_c^2 \rangle = \frac{1}{2\pi L} \int_0^{2\pi} \int_0^L \dot{w}_c^H \dot{w}_c dx d\theta \quad (37)$$

where $\langle w_c \rangle$ is the radial displacement, \dot{w}_c is the radial velocity, the brackets $\langle \rangle$ denotes the spatial average and $()^H$ denotes the Hermitian transpose operator. The kinetic energy of the cylindrical shell due to radial motion is then obtained by $E_k = \frac{1}{2} M \dot{w}_c^2$, where M is the cylinder mass. At the resonant modes, the total energy is twice the kinetic energy which can be obtained by $E = E_k$ (Lyon 1995).

Figures 9 and 10 present the energy levels due to radial motion of the fluid-loaded cylinder obtained analytically and from an SEA model, for the fluid-loaded cylinder with rigid and flexible end plates, respectively. The energy levels obtained analytically were spatially and frequency averaged. The difference in amplitudes in the energy levels between the two figures is attributed to the axisymmetric excitation of the rigid and flexible end plates. For the case of rigid end plates, the cylinder axial modes are predominantly excited which indirectly excites the bending (radial) modes due to the coupling effect by Poisson’s ratio. For the case of flexible end plates, both the axial and bending cylinder modes are directly excited. The results obtained analytically converge to those from the SEA model at higher frequencies, corresponding to around 700Hz for the structure with rigid end plates and 300Hz for the flexible end plates. Below these frequencies, the use of SEA to predict the mean energy levels is not valid.

SEA parameters

Key SEA parameters corresponding to the modal density and coupling loss factors from the SEA model developed in the VA-One software are observed in what follows. The modal density of the cylinder for the radial and axial modes is presented in Fig. 11. The peak in the modal density for the radial modes at 267.5 Hz occurs at the ring frequency of the cylinder, given by $f_r = c_L / 2\pi a$ where c_L is the longitudinal wave speed. Below the ring frequency, the cylinder dynamic response is influenced by the curvature of the shell. Above the ring frequency, the modal density of the cylinder for the radial modes approaches that of a flat plate. The axial modes occur at widely spaced intervals over the frequency spectrum thus their effect on the modal density is very small.

The coupling loss factor is a parameter uniquely associated with SEA and describes the energy transmitted from one subsystem to another. The coupling loss factors between the cylinder and flexible end plates are shown in Fig. 12. The coupling loss factor between the cylinder and driven plate are significantly higher than between the cylinder and receiving plate. A dip in the coupling loss factor from the cylinder to the receiving plate occurs at the ring frequency. Above the ring frequency, the coupling loss factor values of the cylinder/plate structure asymptotes to that of an equivalent plate/plate structure (Tso and Hansen 1997).

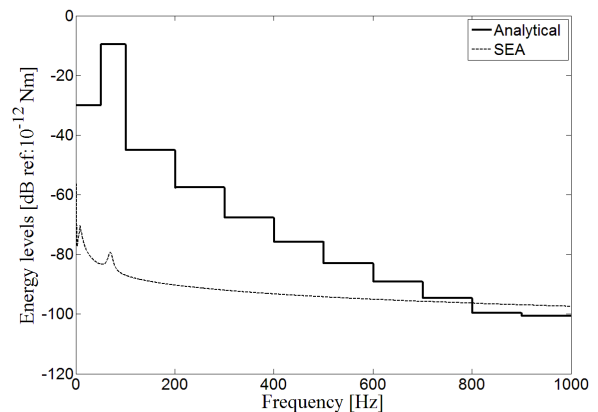


Figure 9. Energy levels due to radial motion of the fluid-loaded cylinder closed by rigid end plates

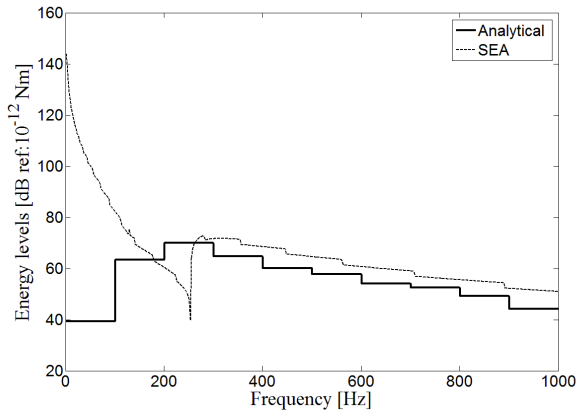


Figure 10. Energy levels due to radial motion of the fluid-loaded cylinder closed by flexible end plates

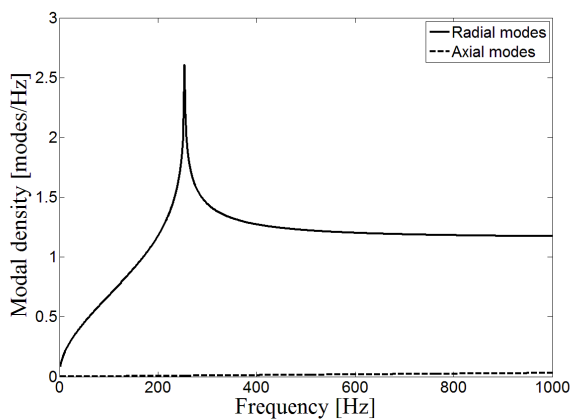


Figure 11. Modal density of the cylinder

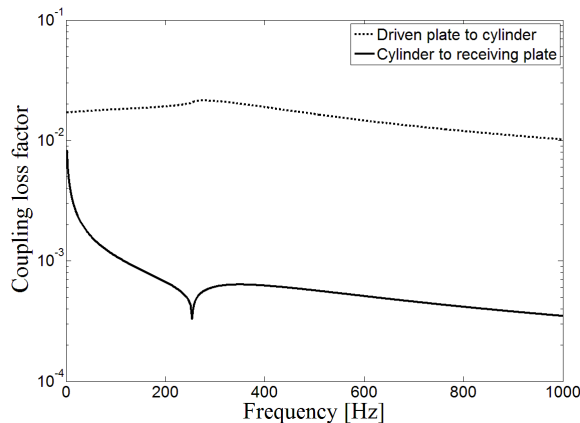


Figure 12. Coupling loss factors between the cylinder and flexible end plate subsystems

SUMMARY

The work presented here uses a combination of deterministic and statistical approaches to predict the dynamic responses of a fluid-loaded coupled cylinder/plate structure. A cylindrical shell closed by either rigid or flexible circular plates was modelled. The acoustic pressure due to the fluid loading acting normal to the surface of the shell was approximated using an infinite model. The axial and radial displacements of the

cylindrical shell were analytically obtained and validated using results from a fully coupled FE/BE numerical model. The spatially and frequency averaged energy due to radial motion of the cylindrical shell obtained analytically was then compared with results obtained from an Statistical Energy Analysis (SEA) numerical model. For this simple structure, good agreement between the energy levels obtained from an analytical model and an SEA numerical model was observed at higher frequencies.

ACKNOWLEDGEMENTS

The authors gratefully acknowledge the financial aid provided by Australian Acoustical Society NSW Division to attend the Acoustics 2012 conference.

REFERENCES

Caresta, M & Kessissoglou, NJ 2011, Reduction of hull-radiated noise using vibroacoustic optimization of the propulsion system, *Journal of Ship Research*, vol. 55, no. 3, pp. 149-162.

Cotoni, V, Shorter, P & Langley, RS 2007, Numerical and experimental validation of the hybrid finite element-statistical energy analysis method, *Journal of the Acoustical Society of America*, vol. 122, no. 1, pp. 259-270.

Fahy, FJ 1994, Statistical energy analysis: a critical overview, *Philosophical Transactions of the Royal Society of London, Series A*, vol. 346, pp. 431-447.

Flügge, W 1973, *Stresses in shells, second edition*, Springer-Verlag, New York.

Fuller, CR & Fahy, FJ 1982, Characteristics of wave propagation and energy distribution in cylindrical elastic shells filled with fluid, *Journal of Sound and Vibration*, vol. 81, no. 4, pp. 501-518.

Huang, DT & Soedel, W 1993, Natural frequencies and modes of a circular plate welded to a circular cylindrical shell at arbitrary axial positions, *Journal of Sound and Vibration*, vol. 162, no. 3, pp. 403-427.

Irie, T, Yamada, G & Muramoto, Y 1984, Free vibration of joined conical-cylindrical shells, *Journal of Sound and Vibration*, vol. 95, no. 1, pp. 31-39.

Junger, MC & Feit, D 1986, *Sound, structures and their interaction*, MIT Press, Cambridge.

Langley, RS & Bremner, P 1999, A hybrid method for the vibration analysis of complex structural-acoustic systems, *Journal of the Acoustical Society of America*, vol. 105, no. 3, pp. 1657-1671.

Langley, RS & Cordioli, JA 2009, Hybrid deterministic-statistical analysis of vibro-acoustic systems with domain couplings on statistical components, *Journal of Sound and Vibration*, vol. 321, no. 3-5, pp. 893-912.

Leissa AW 1993, *Vibration of shells*, American Institute of Physics, New York .

Lyon, RH & DeJong, RG 1995, *Theory and Application of Statistical Energy Analysis, second edition*, Butterworth-Heinemann, Boston.

Mace, BR 1994, On the Statistical Energy Analysis hypothesis of coupling power proportionality and some implications for its failure, *Journal of Sound and Vibration*, vol. 178, pp. 95-112.

Manning, JE 2002, Statistical Energy Analysis of fluid-filled piping vibrations and acoustics, *Proceedings of IMECE2002: ASME 2002 International Mechanical Engineering Congress and Exposition*, New Orleans, Louisiana, pp. 97-103

- Photiadis, DM 1990, The propagation of axisymmetric waves on a fluid-loaded cylindrical shell, *Journal of the Acoustical Society of America*, vol. 88, no. 1, pp.239-250.
- Sandman, BE 1976, Fluid loading influence coefficients for a finite cylindrical shell, *Journal of the Acoustical Society of America*, vol. 60, no. 6, pp. 1256-1264.
- Scott, JFM 1988, The free modes of propagation of an infinite fluid-loaded thin cylindrical shell, *Journal of Sound and Vibration*, vol. 125, no. 2, pp. 241-280.
- Stepanishen, PR 1982, Modal coupling in the vibration of fluid-loaded cylindrical shells, *Journal of the Acoustical Society of America*, vol. 71, no. 4, pp. 813-823.
- Tso, YK & Hansen, CH 1995, Wave propagation through cylinder plate junctions, *Journal of Sound and Vibration*, vol. 186, no. 3, pp. 447-461.
- Tso, YK & Hansen, CH 1997, An investigation of the coupling loss factor for a cylinder/plate structure, *Journal of Sound and Vibration*, vol. 199, no. 4, pp. 629-643.
- Zhang, XM 2002, Frequency analysis of submerged cylindrical shells with the wave propagation approach, *International Journal of Mechanical Sciences*, vol. 44, no. 7, pp. 1259-1273.

APPENDIX

For the axisymmetric case in which only the $n=0$ circumferential modes are excited, the internal cylindrical forces and moments per unit length of shell circumference are given by (Flügge 1973)

$$F_{x,c} = -\frac{Eh}{1-\mu^2} \left(\frac{\partial u_c}{\partial x} + \frac{\mu}{a} w_c - \beta^2 \frac{\partial^2 w_c}{\partial x^2} \right) \quad (\text{A1})$$

$$F_{r,c} = \frac{Eh^3}{12(1-\mu^2)} \left(\frac{\partial^3 w_c}{\partial x^3} - \frac{1}{a} \frac{\partial^2 u_c}{\partial x^2} \right) \quad (\text{A2})$$

$$M_c = -\frac{Eh^3}{12(1-\mu^2)} \left(\frac{\partial^2 w_c}{\partial x^2} - \frac{1}{a} \frac{\partial u_c}{\partial x} \right) \quad (\text{A3})$$

For the circular plate internal forces and moments are

$$F_{x,p} = -D_p \left(\frac{\partial^3 w_p}{\partial r^3} + \frac{1}{a_i} \frac{\partial^2 w_p}{\partial r^2} - \frac{1}{a_i^2} \frac{\partial w_p}{\partial r} \right) \quad (\text{A4})$$

$$F_{r,p} = \frac{E_p h_p}{1-\mu_p^2} \left(\frac{\partial u_p}{\partial r} + \frac{\mu_p}{a_i} u_p \right) \quad (\text{A5})$$

$$M_p = D_p \left(\frac{\partial^2 w_p}{\partial r^2} + \frac{\mu_p}{a_i} \frac{\partial w_p}{\partial r} \right) \quad (\text{A6})$$

$a_i = a_1$ for the inner circular plate at $x=0$. $a_i = a_2$ for the annular plate at $x=0$. $a_i = a$ for the circular plate at $x=L$